

FDINET: Protecting against DNN Model Extraction using Feature Distortion Index

Hongwei Yao, Zheng Li, Haiqin Weng, Feng Xue, Kui Ren *Fellow, IEEE*, Zhan Qin [†]

Abstract—Machine Learning as a Service (MLaaS) platforms have gained popularity due to their accessibility, cost-efficiency, scalability, and rapid development capabilities. However, recent research has highlighted the vulnerability of cloud-based models in MLaaS to model extraction attacks. In this paper, we introduce FDI_{NET}, a novel defense mechanism that leverages the feature distribution of deep neural network (DNN) models. Concretely, by analyzing the feature distribution from the adversary’s queries, we reveal that the feature distribution of these queries deviates from that of the model’s training set. Based on this key observation, we propose Feature Distortion Index (FDI), a metric designed to quantitatively measure the feature distribution deviation of received queries. The proposed FDI_{NET} utilizes FDI to train a binary detector and exploits FDI similarity to identify colluding adversaries from distributed extraction attacks. We conduct extensive experiments to evaluate FDI_{NET} against six state-of-the-art extraction attacks on four benchmark datasets and four popular model architectures. Empirical results demonstrate the following findings: (1) FDI_{NET} proves to be highly effective in detecting model extraction, achieving a **100% detection accuracy** on DFME and DaST. (2) FDI_{NET} is highly efficient, using just 50 queries to raise an extraction alarm with an **average confidence of 96.08%** for GTSRB. (3) FDI_{NET} exhibits the capability to identify colluding adversaries with an accuracy **exceeding 91%**. Additionally, it demonstrates the ability to detect two types of adaptive attacks.

Index Terms—Model extraction, model stealing, Feature Distortion Index.



1 INTRODUCTION

As the performance of deep neural networks (DNN) remarkably improves, DNN has been widely used in various fields (e.g., image recognition and natural language processing). However, the construction of high-performance DNN models requires tremendous amounts of training data and computational resources, making it challenging for end-users to create their own private models. Therefore, many companies choose to deploy DNN models to Cloud Service Providers (CSP) in order to offer online paid services through Machine Learning as a Service (MLaaS) [1]. Recent reports even predict a remarkable economic boost of 21.72 billion dollars in the MLaaS market [2]. Unfortunately, the value associated with these models also leads to the emergence of model extraction attacks (also known as model stealing attacks) [3], [4].

In MLaaS, only the CSP has access to the parameters and architecture of the cloud-based model. The clients can only interact with the model through a public API. While the cloud-based model may appear as a black-box to clients, it is still possible for a malicious client to interact with the model and replicate its behavior using input-output pairs. This poses a significant risk of privacy breach for the cloud-based models. Recent studies [5], [6], [7], [8] have shown that an adversary can launch model extraction attacks by

querying MLaaS, imitating the behaviors of the target DNN model, and creating a surrogate model. Furthermore, using the extracted surrogate model, the adversary can launch additional attacks, including membership inference attacks [9], adversarial examples [10], [11], [12], [13], and model explanations [14], [15]. Consequently, the protection of cloud-based models against model extraction attacks emerges as a critical issue that demands increased attention.

To enhance the security of MLaaS, there have been growing research efforts on model extraction detection [16], [17], [18], [19]. Existing detection approaches typically involve analyzing query distributions and utilizing statistical tools to identify potentially malicious queries. Although the existing detection approaches have made promising progress, they still have several limitations. One key limitation is that most existing methods rely on strong assumptions about the adversary, which limits their generalizability to different extraction attacks. For example, PRADA [17] is designed specifically to detect adversarial example-based queries, DeepDefense [20] fails to identify synthetic data-based queries. As a result, it remains a challenge to identify the intrinsic characteristics of extraction attacks and develop a generic detection method to identify diverse attacks. Second, existing detectors need to maintain local proxy models [16], historical queries [17], or training points [18]. While these components contribute to detection accuracy, they may fail to identify malicious clients efficiently. Therefore, improving the efficiency of detection methods poses a significant challenge. Furthermore, advanced stealth attacks, such as distributed model extraction attacks, can evade the existing detectors. To the best of our knowledge, there is still no countermeasure to defend against the distributed attack, which adopts multi-clients to launch the same model

- Kui Ren, Zhan Qin and Feng Xue are with School of Cyber Science and Technology, Zhejiang University, and Zhejiang Provincial Key Laboratory of Blockchain and Cyberspace Governance, Hangzhou, China. Zhan Qin is the corresponding author. (E-mail: kuiren@zju.edu.cn, qinzhan@zju.edu.cn, and gkn1fexxx@gmail.com).
- Zheng Li is with the German National Big Science Institution within the Helmholtz Association, Saarbrücken, German (E-mail:zheng.li@cispa.de).
- Hongwei Yao is with School of Cyber Science and Technology, Zhejiang University, Hangzhou, China. (E-mail: yhongwei@zju.edu.cn).

extraction attack. Thus, devising an effective defense to mitigate the impact of advanced stealth attacks is a pressing issue.

To address the aforementioned limitations, we propose FDINET, a generic effective and efficient detector against model extraction attacks that can be easily integrated into MLaaS systems. In order to identify the intrinsic differences between benign and malicious queries, we investigate the attack strategies. Concretely, we analyze the queries submitted by adversaries and make a motivative observation: the feature distribution of the adversaries' queries deviates from that of the training set. We refer to it as "feature distortion," which is a universal characteristic across various model extraction attacks. Based on this observation, we introduce the Feature Distortion Index (FDI), a metric designed to quantitatively measure the feature distribution deviation of received queries. Furthermore, we observe a high degree of FDI similarity among queries generated by the same model extraction strategy. This observation opens up new possibilities for identifying colluding adversaries in distributed extraction attacks. Leveraging this insight, we propose a distributed extraction attack detector with the capability of identifying colluding adversaries. Additionally, we consider the adaptive adversary who knows our defense strategy may correct features before submitting queries to MLaaS. We propose an adaptive attack, namely *Feature Correction*, *FeatC*, to evade our defense.

To validate the efficacy of FDINET, we conduct extensive experiments using four benchmark datasets, namely CIFAR10, GTSRB, CelebA, and Skin Cancer Diagnosis. The evaluation results demonstrate that the proposed FDINET effectively and efficiently reveals malicious clients and identifies colluding adversaries. The major contributions of this paper are summarized as follows:

- 1) **Proposal of Feature Distortion Index (FDI):** We propose a novel metric, the FDI, to measure the feature deviation of submitted queries. By utilizing the FDI, we train a binary detector that accurately identifies malicious queries.
- 2) **Identifying colluding adversaries:** We propose a distributed model extraction attack in which the adversary controls multiple colluding clients to send queries with a common attack goal. We analyze the FDI similarity of queries and develop a novel classifier that can identify colluding adversaries. This classifier is a pioneering approach in defending against distributed model extraction attacks.
- 3) **Proposal of the adaptive attack, *FeatC*:** In order to assess the robustness of FDINET, we propose an adaptive attack called *FeatC*, specifically designed to bypass our defense mechanism.
- 4) **Extensive experiments and evaluations:** We conduct extensive experiments to evaluate the performance of FDINET on four benchmark datasets and four popular model architectures. The results demonstrate the effectiveness and efficiency of FDINET in detecting malicious queries. Additionally, our approach is robust that achieves high performance in identifying colluding adversaries and two types of adaptive attacks.

2 RELATED WORKS

2.1 Model Extraction Attacks

The concept of model extraction and the demonstration of its feasibility of stealing intellectual property from private models on commercial MLaaS was initially proposed by Tramèr *et al.* [3]. The main principle of model extraction is to replicate the behavior and functionality of a black-box victim model by analyzing query submissions and their corresponding outputs. In this context, the selection of representative data plays a crucial role in determining the efficiency of model extraction attacks. According to the strategy of sample selection, extraction attacks can be categorized into:

Surrogate data-based schemes (\mathcal{A}_{sur}). In this scenario, the adversary possesses a comprehensive surrogate dataset, such as ImageNet and Flickr, which consists of both problem domain (PD) and non-problem domain (NPD) samples. To enhance the efficiency of query selection, the adversary commonly employs active learning strategies (e.g., Knock-off [28], ActiveThief [29], PAC-based active extraction [30], CopycatCNN [31], Bert Stealing [7], and GNN Stealing [32]).

Adversarial example-based schemes (\mathcal{A}_{adv}). The adversary is assumed to have access to a limited number of the problem domain data. In this scenario, the adversary crafts adversarial examples using primitive data, intending to approximate the decision boundary of the target model (e.g., Jacobian-based Augmentation (JBA) [10], T-RND [17], DualCF [33], and Cloud-Leak [34]).

Synthetic data-based schemes (\mathcal{A}_{syn}). In this scenario, the adversary employs a generative model to craft large-scale synthetic samples. For example, Black-box Ripper [35], Data-free Substitute Training (DaST) [11], Data-free Model Extraction (DFME) [36], DFMS-HL [37], MEGEX [38] and MAZE [39].

Hybrid schemes (\mathcal{A}_{hyb}). The idea behind hybrid schemes is to improve the effectiveness and efficiency of the model extraction attack by combining the strengths of each type of attack and mitigating their limitations (e.g., InverseNet [40], DivTheft [41]).

Since the \mathcal{A}_{hyb} scenario is the combining of other scenarios, we focus on \mathcal{A}_{sur} , \mathcal{A}_{adv} , and \mathcal{A}_{syn} adversaries in this study. It should be noted that those attacks compass a wide range of cutting-edge techniques, covering diverse attack scenarios.

2.2 Defenses against Model Extraction Attacks

The countermeasures against model extraction attacks can be categorized into real-time defense and post-stealing defense. Real-time defense aims to detect and prevent the extraction process when the stealing action is in-progress. On the other hand, post-stealing defense strategies utilize copyright verification techniques, such as DNN Watermarking [42], [43], DNN Fingerprinting [44], [45], [46], or Dataset Inference [47], [48], [49], [50], to verify the ownership of the potentially stolen model.

This paper focuses on real-time model extraction defense, which comprises two primary branches of techniques: passive defense and active defense schemes. To provide a comprehensive overview and comparison of the those defense methods, we present a taxonomy of these techniques

TABLE 1
Taxonomy of real-time model extraction defense approaches.

Method	Type	Support Outputs		Defending Capability			Dummy Query	Feature-corrected Query (Ours)	Distributed Attack (Ours)
		Hard-label	Soft-label	\mathcal{A}_{sur}	\mathcal{A}_{adv}	\mathcal{A}_{syn}			
Kariyappa <i>et al.</i> [21]'2020	Active	x	✓	✓	✓	x	✓	x	x
Zheng [22], [23]'2022	Active	x	✓	✓	x	x	x	x	x
Tribhuvanesh <i>et al.</i> [24]'2020	Active	x	✓	✓	✓	x	x	x	x
Adam <i>et al.</i> [25]'2022	Active	x	✓	✓	✓	✓	x	x	x
Kariyappa <i>et al.</i> [26]'2020	Active	x	✓	✓	✓	x	x	x	x
Kesarwani <i>et al.</i> [16]'2018	Passive	✓	✓	✓	✓	x	x	x	x
Juuti <i>et al.</i> [17]'2019	Passive	✓	✓	x	✓	x	✓	x	x
Zhang <i>et al.</i> [19]'2021	Passive	✓	✓	x	✓	✓	x	x	x
Pal <i>et al.</i> [27]'2021	Passive	✓	✓	✓	✓	✓	x	x	x
Lee <i>et al.</i> [20]'2022	Passive	✓	✓	✓	x	x	x	x	x
FDINET (Ours)	Passive	✓	✓	✓	✓	✓	✓	✓	✓

in Table 1. In the following paragraphs, we will discuss those two branches of methods.

Passive defense. The passive defense approach aims to detect and interrupt malicious actions by monitoring and analyzing the distribution (e.g., abnormal distributions, significant information gain) of incoming queries [16], [17], [19], [20], [27]. PRADA [17] keeps track of the minimum L2-norm distance between last sample and previous samples for each client to detect the adversary. Since PRADA is based on the assumption that samples submitted by an adversary deviate from a normal (Gaussian) distribution, it fails to identify the queries fit with a normal distribution. Extraction Monitor (EM) [16] employs local proxy models to quantify the extraction status of an individual client. However, EM has two main drawbacks: (1) employing local proxy models results in high memory consumption that degrades the efficiency of MLaaS, (2) large false alarms may be raised for the benign client.

Active defense. The active defense approach involves adding perturbation to the victim model's output [21], [22], [23], [24], [26], [51], [52], [53], [54], [55]. Orekondy *et al.* propose Prediction Poisoning [24], which adds utility-constrained perturbations on the posteriors. The perturbations maximize the angular deviation between the gradient of the poisoned posteriors and that of the victim model. Zheng *et al.* propose BDPL [22], [23], which exploits Differential Privacy to add obfuscating noises on the prediction logits.

Passive defense strategies are the main focus of this paper due to the inherent limitations of active defense methods. Active defense approaches rely on strong assumptions about the output forms, which give rise to two significant drawbacks. Firstly, introducing perturbed probabilities may negatively impact the utility of cloud-based models. Secondly, these methods are not applicable in scenarios where hard-label outputs are used instead of probability vectors. Therefore, this paper primarily discusses the utilization of passive defense strategies.

3 PRELIMINARIES

A Deep Neural Network (DNN) model is a function $F : \mathcal{X} \rightarrow \mathcal{Y}$ parameterized by a set of parameters, where $\mathcal{X} \in \mathbb{R}^d$ denotes the d -dimensional feature space and \mathcal{Y}

represents the output space. For an online MLaaS application, the private DNN model F_V is first trained by the developer using enormous training data \mathcal{D}_{train} to achieve a high accuracy on testing set \mathcal{D}_{test} and then deployed to the CSP. Through querying prediction API using a pay-as-you-go manner, the client can access prediction probabilities $F_V(x)$ for any given input data x . The goal of model extraction is to create a surrogate model F_S that replicates the functionality of the black-box victim model F_V .

3.1 Attack Capabilities

In real-world scenarios, the adversary is typically restricted from accessing the inner operations of cloud-based models, including private training data, model architecture, and model parameters. However, the adversary can still engage with the black-box model through the submission of queries and the retrieval of prediction probabilities via the publicly accessible API interface.

Adversary's query set. We consider three types of adversaries as mentioned in Section 2.1 (i.e., \mathcal{A}_{sur} , \mathcal{A}_{adv} , and \mathcal{A}_{syn}). For \mathcal{A}_{sur} , the incoming queries come from PD and NPD natural images. For \mathcal{A}_{adv} , the submitted queries contain adversarial examples. For \mathcal{A}_{syn} , the malicious queries are synthetic data from a generator.

Colluding adversaries. Within the context of MLaaS, adversaries may employ multiple clients $N(N > 1)$ to enhance the stealthiness of their attacks and bypass request limitations. These colluding clients, under the control of a central adversary, collaborate to carry out model extraction attacks using similar query selection strategies, all working towards a common objective. In this paper, we refer to these clients as colluding adversaries.

Adaptive adversary. In the context of model extraction, we must consider the presence of an adaptive adversary who possesses knowledge of the defense methods employed. This adversary can modify their query submission strategy to enhance the stealthiness of the extraction process. In this paper, we focus on two types of adaptive adversaries: (1) *Dummy Query*: This adaptive method, proposed by PRADA [17], involves generating dummy queries that do not contribute to the model extraction process. These queries are designed to maintain a normal distribution within a sequence of historical queries, thereby evading detection.

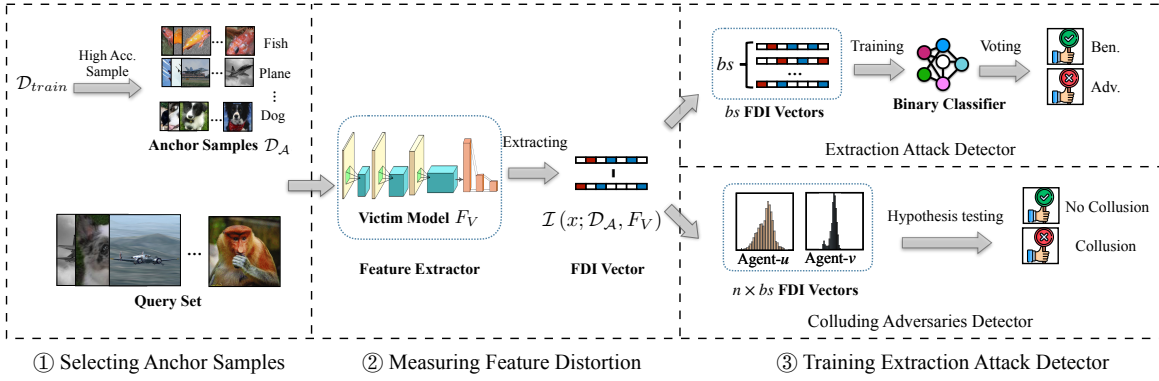


Fig. 1. Overview the pipeline of FDINET. In the first step, we select K anchor samples for each class c (airplane in figure). In the next step, we measure feature distortion to obtain FDI vector for each inspected sample. Finally, the extracted FDI vector is used to create a binary extraction attack detector and a colluding adversaries detector.

(2) *Feature Correction*: To evade detection, the adversary employs an auxiliary encoder, denoted as \hat{F} , which is a pre-trained encoder drawn from model zoo. This auxiliary encoder is used to correct the query's feature maps before submitting them to the MLaaS system. We will discuss the detail of *Feature Correction* in Section 4.4.

3.2 Defense Objective and Assumptions

Protection of user data is of utmost importance in the MLaaS platform. It is imperative for a secure MLaaS system to prioritize the confidentiality of user models.

Defense objective. The defender acts as a crucial intermediary between the CSP and clients, with the main goal of detecting and preventing extraction actions. It aims to create a powerful extraction attack detector \mathcal{C} that can distinguish between benign and malicious queries. As a result, the goal of defender is:

$$\max_x P_{(x \in \mathcal{D}_{adv})} \mathbb{1}[\mathcal{C}(F_V; x) = 1] + P_{(x \in \mathcal{D}_{test})} \mathbb{1}[\mathcal{C}(F_V; x) = 0], \quad (1)$$

where \mathcal{D}_{adv} is query set of adversary, \mathcal{C} is the extraction attack detector. Additionally, the defender aims to evaluate the performance of detector using the following metrics: (1) *effectiveness*, the detector is expected to effectively identify various types of extraction attacks. (2) *efficiency*, for the low-latency MLaaS platform, the defense algorithm should immediately raise extraction alarms using only a few queries. (3) *robustness*, the defender has the ability to resist stealthy attacks, such as distributed attacks, as well as adaptive attacks.

Defending assumptions. We consider the attack-agnostic scenario, where the defender has no prior knowledge of sample selection strategies. Besides, the attack model architecture, training mechanism, and relationship between clients are unknown to the defender. We suppose that the defender knows developer's private training data \mathcal{D}_{train} and has access to the feature maps of victim model F_V . The PROFEDI is generic and flexible since it makes no assumptions about the adversary, the DNN model, and the developer's private training data. This results in its defense capability of identifying extraction attacks in all scenarios, including \mathcal{A}_{sur} , \mathcal{A}_{adv} , and \mathcal{A}_{syn} .

4 METHODOLOGY

As shown in Figure 1, the detection process of FDINET includes the following phases: (1) selecting anchor samples, (2) measuring feature distortion, (3) training extraction attack detector. In the first phase, we select high prediction confidence data from the training set as anchor samples. Subsequently, the feature space distances between each inspected sample and the anchor samples are calculated to generate the FDI vector. Finally, the extracted FDI vector is employed as an intrinsic feature to train the extraction attack detector.

4.1 Selecting Anchor Samples

The adversary selects and/or crafts samples to query the public API, then uses the prediction results as labels to train a clone model. Intending to extract more information from the cloud-based model, the adversary explores enormous input space to increase the diversity of queried samples. Therefore, the feature distributions of sample submitted by an adversary deviate from benign training data. This phenomenon motivates us to design an effective metric to measure the feature distributions deviation between received query and training data.

The first step toward measuring feature space deviation is to select anchor samples. To ensure the selected representative samples lie in the center, we select K high-confidence data from training set as anchor samples for each class. It should be noted that these anchor samples lie at the center of each class, encapsulating the statistical features of the benign query set. Formally, for each class c , the selected samples are denoted as $\{(x_{c,j}, c)\}_{j=1}^K \in \mathcal{D}_{anc}$. Afterwards, we use the selected anchor sample $(x_{c,j}, c)$ to extract feature maps $F_V^l(x_{c,j})$ for layer l .

4.2 Measuring Feature Distortion

The observed deviation in feature distributions between an inspected sample and the anchor samples is referred to as the feature distortion of the inspected sample. To quantitatively measure this feature distortion, we introduce a novel metric called the Feature Distortion Index (FDI). The FDI serves as a quantitative measure to assess the extent of

feature distortion in the inspected sample compared to the anchor samples. Formally, the FDI is defined as follows:

Definition 4.1 (*Feature Distortion Index*). Given a victim model F_V , an anchor set \mathcal{D}_{anc} , the feature distortion index for an inspected sample (x, c) is defined as:

$$\mathcal{I}_j^l = d\left(F_V^l(x) - F_V^l(x_{c,j})\right) \quad \text{s.t. } x_{c,j} \in \mathcal{D}_{anc}, \quad (2)$$

where $F_V^l(x)$ denotes the output feature of F_V for layer l , d indicates the l_2 -norm in our paper, and c is the label of x predicted by F_V .

Given a victim model F_V , we extract a total of L layer feature maps (i.e., $l \in \{1, \dots, L\}$). We then concatenate all \mathcal{I}^l to obtain a $(K \times L)$ -dimension FDI vector. For example, for VGG19 of task CIFAR10, we select $K = 100$ anchor samples and extract $L = 5$ layer feature maps to obtain a (5×100) -dimension FDI vector $\mathcal{I}(x, c; \mathcal{D}_{anc}, F_V)$.

4.3 Training Extraction Attack Detector

In this section, we employ the extracted FDI vector as the inputs to (1) construct a binary classifier to detect extraction queries, (2) perform hypothesis tests to identify colluding adversaries.

TABLE 2
Architecture of binary classifier \mathcal{C}

Index	Layer Type	Weight
1	Linear	$[K \times L, 256]$
2	Linear	$[256, 32]$
3	Linear	$[32, 2]$
4	Softmax	-

4.3.1 Detecting Extraction Attacks

Table 2 illustrates the architecture of \mathcal{C} . The binary classifier, takes in a $(K \times L)$ -dimension FDI vector as input and produces a 2-dimensional probability vector as output.

Training. In order to train \mathcal{C} , we adopt the training strategy commonly used in Out-of-Distribution detection. Specifically, we gather a positive dataset and a negative dataset, which are utilized during the training process. In this paper, we utilize the \mathcal{D}_{train} as the negative dataset and collect an auxiliary dataset \mathcal{D}_{aux} as the positive dataset. The selection of \mathcal{D}_{aux} will be discussed in Section 5.1.3.

Evaluation. Identifying malicious clients based on a single query can be challenging due to its low information entropy. To overcome this limitation, we introduce a majority voting algorithm that utilizes a batch size of bs queries to detect malicious clients. In this approach, for each submitted query with a batch size of bs samples, we calculate the average confidence score of the predictions and utilize it as an indicator to determine the maliciousness of the client.

$$ac = \frac{1}{bs} \times \sum_{i=1}^{bs} \arg \max \mathcal{C}(\mathcal{I}(x, c; \mathcal{D}_{anc}, F_V)), \quad (3)$$

where bs is the length of sequence and $ac \in [0, 1]$ is a confidence score.

Algorithm 1: Training and Prediction of \mathcal{C}

Input: Victim model F_V , negative set \mathcal{D}_{train} , positive set \mathcal{D}_{aux} , anchor set \mathcal{D}_{anc} , received query $x_i (i \leq bs)$

Output: Majority voting score ac

```

1 FUNCTION Training:
2 for  $(x, y) \leftarrow \mathcal{D}_{train} \cup \mathcal{D}_{aux}$  do
3    $c = F_V(x)$ 
4    $\mathcal{I} = [\mathcal{I}_1^1, \dots, \mathcal{I}_K^1, \dots, \mathcal{I}_1^L, \dots, \mathcal{I}_K^L]$ 
5    $\mathcal{C} = \arg \min_c \mathcal{L}_{\text{cross-entropy}}(\mathcal{I}, y)$  // training step
6 end
7 FUNCTION Prediction:
8 score = 0
9 for  $i \leftarrow bs$  do
10   $c_i = F_V(x_i)$ 
11   $\mathcal{I} = [\mathcal{I}_1^1, \dots, \mathcal{I}_K^1, \dots, \mathcal{I}_1^L, \dots, \mathcal{I}_K^L]$ 
12  score+ = arg max  $\mathcal{C}(\mathcal{I})$ 
13 end
14 ac = score/bs
15 return ac
```

Finally, we adopt a threshold τ_1 to determine whether the queries come from malicious or benign clients. Note that if confidence score ac high than threshold τ_1 , the query is predicted as extraction attack. The training and prediction of \mathcal{C} are described in Algorithm 1.

4.3.2 Identifying Colluding Adversaries

In this section, we first define distributed model extraction attacks and introduce our method to identify colluding adversaries.

Distributed extraction attack. Given an MLaaS platform with $M = \{1, 2, \dots, M\}$ clients, a central adversary controls a set of $N (2 \leq N \leq M)$ clients. The central adversary adopts sample selection strategies (e.g., \mathcal{A}_{sur} , \mathcal{A}_{adv} , and \mathcal{A}_{syn}) to build a query set and distributes them to each client. The distributed attack is stealthy since each controlled agent only has a small overhead that is easy to evade request limitations.

Colluding adversaries detection. We observe a significant level of FDI similarity among queries that are generated using the same model extraction attack. This key observation motivates us to detect colluding adversaries using FDI similarity.

In order to determine if two examined clients, u and v , are colluding adversaries, our approach involves collecting a set of $n \times bs$ historical queries from each client. Subsequently, we extract their FDI vectors and perform two-sample hypothesis tests for further analysis as follows:

Proposition 4.1 (*Two-sample Hypothesis Tests*). Given two inspected clients u and v , and their $n \times bs$ FDI vectors \mathcal{I}_u and \mathcal{I}_v , the null hypothesis can be expressed as: $\mathcal{H}_0 : \mu_u = \mu_v$, while the alternative hypothesis is expressed as $\mathcal{H}_a : \mu_u \neq \mu_v$. Though calculating the test statistic $\mathbf{t} = (\bar{x}_1 - \bar{x}_2) / s_p \left(\sqrt{\frac{1}{|\mathcal{I}_u|} + \frac{1}{|\mathcal{I}_v|}} \right)$, we can obtain its p-value, where \bar{x}_1 and \bar{x}_2 are means of samples, s_p indicates variance.

Finally, we select a threshold τ_2 chosen for statistical significance (usually $\tau_2 = 0.05$) for testing. If the calculated p-value is below τ_2 , then the null hypothesis \mathcal{H}_0 is rejected in favor of the alternative hypothesis \mathcal{H}_a . In this case, it indicates that clients u and v are not colluding adversaries.

4.4 Adaptive Attacks

An adaptive adversary who knows FDINET may potentially modify attack strategies to evade our detection. In this section, we assume that the adaptive adversary has a mini-batch of substitute anchor samples and an auxiliary encoder \hat{F} drawn from the model zoo. We proposed *Feature Correction (FeatC)*, an adaptive attack that utilizes an auxiliary encoder to make the query similar to anchors samples in feature maps. Formally, the adaptive adversary locally perturbrates x using loss function \mathcal{L} :

$$\mathcal{L}(x; \hat{F}, \hat{x}) = \|\hat{F}^l(x + \delta) - \hat{F}^l(\hat{x})\|_2^2 \quad (4)$$

s.t. $F_V(x) = F_V(\hat{x}), \delta < \epsilon,$

where \hat{F} is a pre-trained feature extractor drawn from model zoo and \hat{x} denotes auxiliary anchor sample from victim training data \mathcal{D}_{train} . Through generating feature-corrected queries, the adaptive adversary intends to bypass our detection. Since *FeatC* exploits the full knowledge of our defense mechanism, we believe *FeatC* is a strong adaptive attack against FDINET.

5 EXPERIMENTS

In this section, we conduct extensive experiments to validate the performance of FDINET against six advanced model extraction attacks, covering four different deep learning systems. We begin by introducing the experimental setup in Section 5.1. Subsequently, we evaluate the performance of FDINET against extraction attacks in Section 5.2 and distributed attacks in Section 5.3. Additionally, we conduct ablation studies in Section 5.4 and explore the adaptive attacks in Section 6.1. All experiments are performed on an Ubuntu 20.04 system equipped with a 96-core Intel CPU and four Nvidia GeForce GTX 3090 GPU cards. The machine learning algorithm is implemented using PyTorch v1.10.

5.1 Experimental Setup

5.1.1 Datasets and Victim Models

TABLE 3
Datasets and victim models.

Dataset	Model	Acc.(%)	Scenario
CIFAR10	VGG19	87.73	General Visual Recognition
GTSRB	MobileNetV2	90.99	Traffic Sign Recognition
CelebA	DenseNet121	93.49	Face Recognition
Skin Cancer	ResNet50	98.52	Disease Diagnosis

Our method is assessed on four benchmark datasets: CIFAR10 [56], GTSRB [57], CelebA [58] *, and Skin Cancer [59]. These datasets cover four distinct deep learning

systems that are commonly employed in security-critical domains: general visual recognition, traffic sign recognition, face recognition, and disease diagnosis. To conduct our experiments, we utilize four different convolutional neural networks: VGG19, MobileNetV2, DenseNet121, and ResNet50. To accommodate the input size of 32×32 , we adjusted the filter size of the first convolutional layer in the original architecture by downsampling. Table 3 presents a summary of the datasets and victim models utilized in our experiments.

5.1.2 Setting of Attack Methods

TABLE 4
Surrogate model's Top-3 accuracy(%) of various model extraction attacks for \mathcal{A}_{sur} , \mathcal{A}_{adv} and \mathcal{A}_{syn} scenarios.

Dataset	\mathcal{A}_{adv}		\mathcal{A}_{sur}		\mathcal{A}_{syn}	
	JBA	T-RND	Knockoff	ActiveThief	DFME	DaST
CIFAR10	54.87	62.61	97.23	95.23	96.98	35.18
GTSRB	26.79	21.65	34.26	33.99	92.73	40.09
CelebA	76.55	76.94	99.85	82.36	92.74	42.84
Skin Cancer	74.44	69.50	94.89	99.48	82.56	61.35

Six advanced model extraction attacks are considered in our experiments, covering three adversarial scenarios, i.e., \mathcal{A}_{adv} , \mathcal{A}_{sur} and \mathcal{A}_{syn} (as mentioned in Section 2.1). For \mathcal{A}_{adv} scenario, we assume the adversary has a mini-batch of victim's training data and employs Jacobian-based Augmentation (JBA) [10] Targeted Randomly Chosen Direction (T-RND) [17] to create extraction query. For \mathcal{A}_{sur} scenario, we follow the experiment setting of Knockoff [28], which assumes the adversary selects queries from a surrogate dataset. Specifically, we adopt CINIC-10 [60], TSRD[†], LFW [61], and BCN20000 [62] as Knockoff and ActiveThief [29]'s surrogate dataset for the tasks of CIFAR10, GTSRB, CelebA and Skin Cancer, respectively. For \mathcal{A}_{syn} scenario, we follow DFME [36] and DaST [11]'s experiment setting that employs a generative model to craft surrogate data as query set. Table 4 provides a summary of the surrogate model's Top-3 accuracy for each attack. Note that those six model extraction attacks compass a wide range of cutting-edge techniques, and their queries cover problem domain data, non-problem domain data, adversarial examples, and synthetic data.

5.1.3 Setting of Defense Methods

In the main paper, we conduct a performance comparison between FDINET, PRADA [17], SEAT [19] and Extraction Monitor [16]. To ensure consistency, we utilize the official implementation of PRADA and make adjustments to the hyperparameter τ_1 in order to achieve a low false positive rate (FPR) on the validation set. Regarding SEAT, we employ the victim model as an encoder and perform fine-tuning for 20 epochs using the Stochastic Gradient Descent (SGD) optimizer with a learning rate of 0.001. Following SEAT's methodology, we select a threshold that yields a low FPR on the validation set. For the Extraction Monitor, we adopt the same architecture as the victim model and treat it as a

*We adopt gender attributes in our experiment.

[†]<http://www.nlpr.ia.ac.cn/pal/trafficdata/recognition.html>

TABLE 5
The DAcc. and FPR of FDINET, PRADA and SEAT to detect against the-state-of-art extraction attacks.

Dataset	Strategy	bs	τ_1	JBA		T-RND		Knockoff		ActiveThief		DFME		DaST	
				DAcc.	FPR	DAcc.	FPR	DAcc.	FPR	DAcc.	FPR	DAcc.	FPR	DAcc.	FPR
CIFAR10	SEAT	50	0.87	9.30	0.20	11.40	0.30	5.80	0.0	5.30	0.0	12.20	0.10	13.90	0.0
		500	0.81	91.00	0.0	90.00	0.0	55.00	0.0	45.00	0.0	75.00	0.0	77.00	0.0
	PRADA	50	0.99	0.0	0.0	0.0	0.0	0.0	0.0	0.0	0.0	0.0	0.0	0.0	0.0
		500	0.97	100.0	36.00	100.0	36.00	28.00	36.00	39.00	36.00	30.00	36.00	19.00	0.0
	FDINET	50	0.47	89.90	4.10	93.10	2.60	80.26	4.10	82.00	2.90	100.0	1.70	98.03	1.80
		500	0.48	91.00	0.0	93.00	0.0	90.00	0.0	92.00	0.0	100.0	0.0	100.0	0.0
GTSRB	SEAT	50	0.90	4.20	4.40	3.80	4.40	8.20	4.20	8.60	4.20	34.20	4.40	43.20	4.40
		500	0.88	74.00	4.00	77.00	4.00	65.00	4.00	55.00	4.00	89.00	4.00	85.00	4.00
	PRADA	50	0.94	0.0	0.0	0.0	0.0	0.0	0.0	0.0	0.0	0.0	0.0	0.0	0.0
		500	0.93	97.00	9.00	97.00	9.00	0.00	9.00	1.00	9.00	1.00	9.00	16.00	9.00
	FDINET	50	0.77	90.30	0.0	90.40	0.0	100.0	0.0	95.60	0.0	100.0	0.0	100.0	0.0
		500	0.78	88.00	0.0	87.00	0.0	100.0	0.0	95.00	0.0	100.0	0.0	100.0	0.0
CelebA	SEAT	50	0.90	5.50	0.0	8.40	0.0	0.0	0.0	0.0	0.0	14.10	0.0	19.30	0.0
		500	0.82	89.00	0.0	79.00	0.0	0.0	0.0	0.0	0.0	79.00	0.0	90.00	0.0
	PRADA	50	0.96	0.0	0.0	0.0	0.0	0.0	0.0	0.0	0.0	0.0	0.0	0.0	0.0
		500	0.95	100.0	6.00	100.0	6.00	3.00	6.00	1.00	6.00	5.00	6.00	9.00	6.00
	FDINET	50	0.33	96.61	0.30	97.10	0.10	83.93	0.30	97.10	0.0	100.0	0.10	100.0	0.20
		500	0.36	95.00	0.0	96.00	0.0	93.00	0.0	93.00	0.0	100.0	0.0	100.0	0.0
Skin Cancer	SEAT	50	0.90	10.20	0.0	8.90	0.0	5.30	0.0	6.00	0.0	4.50	0.0	8.40	0.0
		500	0.82	69.00	2.00	73.00	2.00	62.00	2.00	63.00	2.00	81.00	2.00	87.00	2.00
	PRADA	50	0.93	0.0	0.0	0.0	0.0	0.0	0.0	0.0	0.0	0.0	0.0	0.0	0.0
		500	0.91	98.00	1.00	98.00	1.00	28.00	1.00	26.00	1.00	23.00	1.00	34.00	1.00
	FDINET	50	0.51	92.80	0.0	93.20	0.0	88.70	0.0	89.90	0.0	99.80	0.0	97.40	0.0
		500	0.48	94.00	0.0	94.00	0.0	100.0	0.0	80.00	0.0	100.0	0.0	100.0	0.0

proxy model, as suggested in the original paper. To train the proxy model, we utilize SGD with a learning rate of 0.005 for 2 iterations per batch of submitted queries.

When considering FDINET, we establish the number of anchor samples (K) as 20 for GTSRB, CelebA, and Skin Cancer datasets, whereas for CIFAR10, K is set to 100. We divide the neural network into multiple convolutional blocks and extract 5 layers (i.e., $L = 5$) for all tasks. As for the auxiliary dataset \mathcal{D}_{aux} , we employ the testing set from CINIC-10, TSRD, VGGFace2, and BCN20000 as negative data for CIFAR10, GTSRB, CelebA, and Skin Cancer, respectively. It is important to note that the auxiliary datasets are based on realistic assumptions, and the testing set does not overlap with the surrogate set used by the attacker. To detect distributed attacks, we utilize two-sample hypothesis tests for the two inspected clients, denoted as u and v .

5.1.4 Evaluation Metrics

In the experiments, we utilize five commonly employed metrics to assess the efficacy of our method: Detection Accuracy (DAcc.), False Positive Rate (FPR), Extraction Status (ES), Colluding Detection Accuracy (CDAcc.), and p-value of hypothesis tests. We will discuss the detail of each metric in the following experiments.

5.1.5 Threshold Selection

Achieving optimal DAcc. and FPR in binary classification tasks relies heavily on selecting the right threshold. Nonetheless, this task can be quite challenging. Inspired by previous research [17], we introduce a data-driven threshold selection strategy. Initially, we utilize the validation set \mathcal{D}_{val} to calculate the values of μ_{ac} and σ_{ac} , and subsequently apply the 3σ rule to set $\tau_1 = \mu_{ac} + 3 \times \sigma_{ac}$.

5.2 Detecting Extraction Attacks

In this experiment, we launch extraction attacks and generate 50,000 samples as malicious client's query set \mathcal{D}_{adv} . We evaluate FDINET using DAcc., FPR, and extraction status. The DAcc. serves as a measure of accuracy for detecting malicious queries within the MLaaS system. On the other hand, the FPR quantifies the rate at which negative samples are erroneously classified as positive by the binary detector. It helps evaluate the system's performance in terms of misclassifying negative instances. Additionally, the ES metric evaluates the fidelity between the proxy model and the victim model.

5.2.1 Detection Accuracy and FPR

Table 5 presents a summary of the performance comparison between FDINET, PRADA, and SEAT against six model extraction attacks. In our experiments, we examine two query batch sizes, $bs = 50$ and $bs = 500$. Figure 2 illustrates the ROC curve of our method for detecting extraction queries.

In terms of performance, FDINET outperforms PRADA and SEAT with high DAcc. and low FPR. Specifically, FDINET achieves a DAcc. of **100%** and an FPR close to **0.0** for DFME and DaST with a batch size (bs) of 500. Furthermore, FDINET is capable of identifying malicious clients with just 50 queries. On the other hand, both PRADA and SEAT fail to detect extraction attacks when bs is set to 50. It should be noted that FDINET achieves a lower DAcc. in CIFAR10 for Knockoff and ActiveThief. This is because the surrogate dataset (CINIC-10) used by Knockoff and ActiveThief has some overlap with CIFAR10. In the ablation study, we will explore the effects of threshold τ_1 and batch size (bs) further, which can be found in Section 5.4.

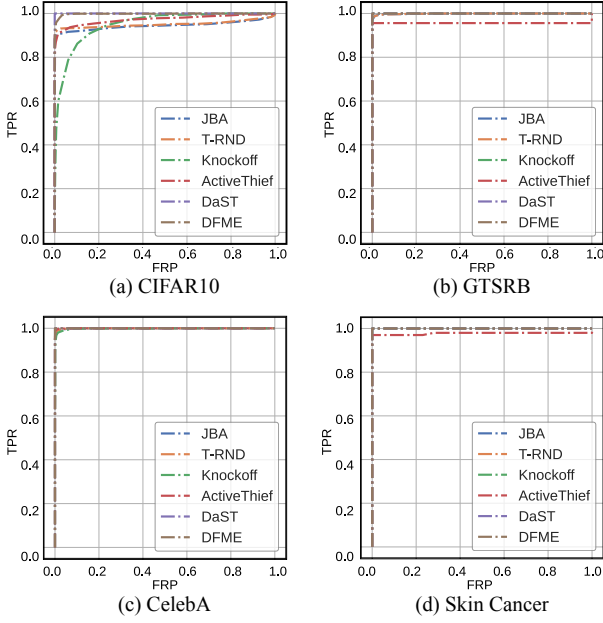


Fig. 2. ROC curve of model extraction attacks detection.

5.2.2 Extraction Status (ES)

ES serves as another important metric for detecting extraction queries. It is a metric introduced by EM [16], which employs information gain to quantify the level of model privacy leakage from the victim model. EM utilizes a local proxy model to monitor the information gain of each client. When the proxy model learns a surrogate model with high fidelity, extraction warnings are sent to the Cloud Service Provider (CSP). Formally, the ES is defined as:

$$es = \frac{100}{|\mathcal{D}_{test}|} \sum_{x \in \mathcal{D}_{test}} \mathbb{1}[F_V(x) = F_{V'}(x)]. \quad (5)$$

Since FDINET doesn't make use of proxy model, we use average confidence (i.e., $(100 \times ac)\%$) as ES for comparison.

Figure 3 depicts the average ES reported by FDINET and EM for both benign and malicious clients. The results demonstrate that FDINET's ES is **below 34.60% for CIFAR10, 44.20% for GTSRB, 17.40% for CelebA, and 9.30% for Skin Cancer**. Additionally, we achieve an average of **96.08% and 84.94% for GTSRB and Skin Cancer**, respectively. On the other hand, FDINET effectively identifies high ES for malicious clients (i.e., JBA, T-RND, Knockoff, ActiveThief, DFME, and DaST). In contrast, EM reports high ES for benign clients due to their significant information gain. Furthermore, the ES of EM is very low for DFME and DaST since these synthetic data samples have low information gain. It is important to note that lower ES is preferable for benign queries, while higher ES is better for malicious queries. Therefore, while EM effectively detects certain extraction attacks, it may also produce considerable false alarms for benign queries.

5.2.3 Memory Costing and Detection Fine-grained

Efficiency is crucial in the context of MLaaS, particularly when dealing with real-time APIs. In the case of security-focused MLaaS, efficiency encompasses two key aspects:

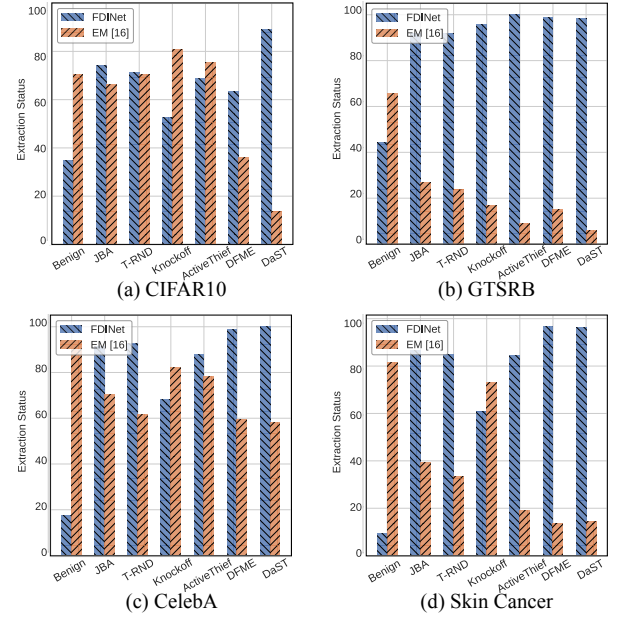


Fig. 3. Results of average Extraction Status for benign and malicious clients (**lower is better for benign clients**). Extraction Status (ES) is a metric proposed by [16] that uses information gain to quantify model privacy leakage from the victim model.

resource consumption and detection fine-grained. To assess our method's efficiency, we compare it with state-of-the-art defense methods.

First, PRADA, relies on calculating the L2 distance between new and previous samples to identify malicious queries. However, this approach necessitates significant memory storage. Additionally, EM requires the maintenance of a local proxy model for each client, resulting in substantial computational overhead. In contrast, our approach, FDINET, is lightweight and flexible. It doesn't depend on historical queries and doesn't make assumptions about the victim model. We conducted an experiment using 50,000 testing queries. The results demonstrate that FDINET achieves a throughput of 838.36 queries on the task of CIFAR10. This showcases the efficiency of FDINET in processing queries promptly and effectively.

Furthermore, as shown in Table 5, FDINET is efficient in identifying extraction queries using only 50 queries. This highlights the efficiency of FDINET in swiftly and accurately detecting adversaries, thereby maximizing the protection of the victim model.

5.3 Detecting Distributed Extraction Attacks

In distributed extraction attack, the adversary distributes malicious queries to $N(N > 1)$ clients. The primary goal of FDINET is not to identify malicious queries, but rather to identify colluding adversaries. To evaluate the performance of FDINET, we simulate an MLaaS system with $M = 100$ clients, each submitting 50,000 queries. Among them, $2 \sim 20$ are colluding adversaries who jointly launch the same extraction attack. In this experiment, we set $bs = 500$ and $n = 100$, with a total of 50,000 samples. For each pair of clients under inspection, denoted as u and v , we extracted their FDI vectors. Subsequently, we conducted two-sample

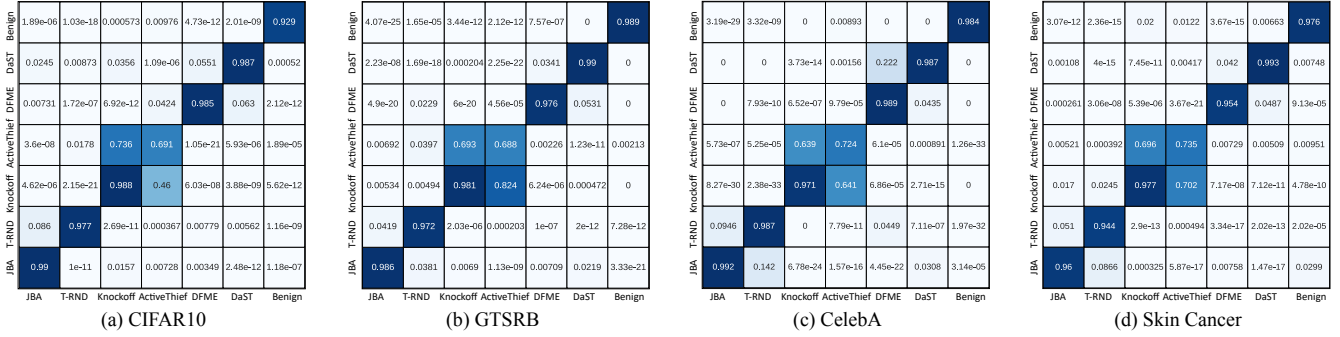


Fig. 4. Illustration of the confusion matrix for average hypothesis tests' p-values over different clients. If the p-value is higher than 0.05, we accept \mathcal{H}_0 , meaning clients u and v are colluding adversaries.

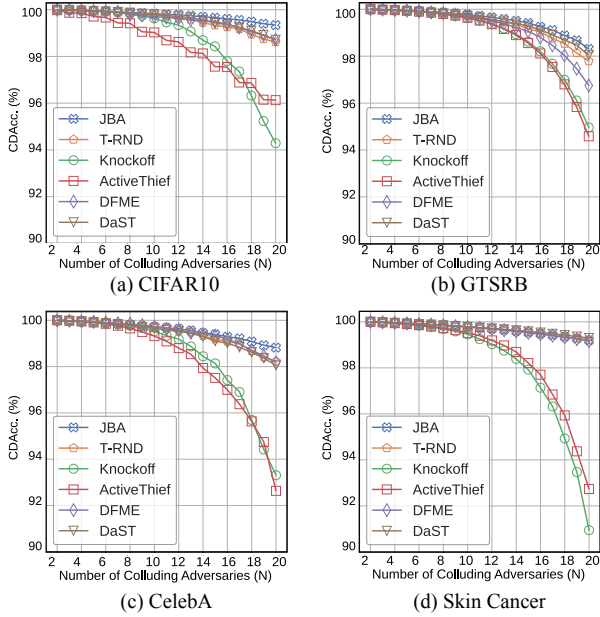


Fig. 5. Performance of colluding adversaries detection for distributed attacks. We consider a 100 clients MLaaS platform. Among them, 2 ~ 20 are colluding adversaries for each attack.

hypothesis tests (as discuss in Proposition 4.1) to determine whether these clients were colluding adversaries. This process allowed us to identify and expose potential collusive behavior among the clients in the MLaaS system. The Colluding Detection Accuracy (CDAcc.) can be formulated as:

$$\text{CDAcc.} = \frac{\sum_{u < v, u \in [1, N], v \in [1, N]} \mathbb{1}[\text{FDINET}(u, v) = J(u, v)]}{C_N^2} \times 100\%, \quad (6)$$

where C is combination formula (i.e., $C_n^m = \frac{n!}{m!(n-m)!}$), J is the judgment function that returns 1 if client u and client v are colluding adversaries. In order to speed up the detection of FDINET, we first use binary detection to filter the benign clients, then setup two-sample hypothesis tests.

Figure 4 depicts the confusion matrix for average hypothesis tests' p-values over different clients. When the p-value exceeds 0.05, we accept the null hypothesis (\mathcal{H}_0), indicating that clients u and v are colluding adversaries. The observation from Figure 4 indicates that FDINET achieves high p-values along the diagonal of the confusion matrix, indicating its effectiveness in identifying colluding adver-

saries. However, our method doesn't performant well in distinguishing between Knockoff and ActiveThief attacks. This challenge arises because both attacks utilize the same surrogate dataset, resulting in similar FDI for these two attacks. Figure 5 demonstrates the effectiveness of FDINET in detecting colluding adversaries within a large-scale MLaaS platform comprising 100 clients. Notably, FDINET achieves an impressive CDAcc. of **over 91%** for all extraction attacks. As Figure 5 illustrates, with the increasing number of colluding adversaries, FDINET can still remain high accuracy for colluding detection. This experiment serves as compelling evidence demonstrating the capability of our method to identify colluding adversaries within a large-scale MLaaS platform effectively.

5.4 Ablation Study

To further understand how different components influence FDINET, we carry out evaluations on two significant factors within our approach, i.e., threshold τ_1 and batch size bs .

5.4.1 Impacts of Threshold

As discussed in Section 5.1.5, the threshold is a critical factor that affects the DAcc., and the process of selecting a suitable threshold is demanding. To shed light on this matter, we conduct an experiment where we employ various thresholds (ranging from 0.2 to 0.8), to observe the trend in detection accuracy. This experiment aims to provide guidance on selecting an optimal threshold that ensures accurate detection for new datasets.

Figure 6 illustrates the impact of thresholds (τ_1) on the DAcc. of FDINET. It can be observed that there is a notable decrease in DAcc. as τ_1 increases, particularly for Knockoff and ActiveThief. This decline in accuracy can be attributed to the fact that the surrogate data used by Knockoff and ActiveThief are derived from natural images, which may have a higher degree of feature overlap with \mathcal{D}_{train} . In our approach, the threshold τ_1 represents the tolerance for abnormal samples in the batch query. By increasing the threshold τ_1 , we can minimize false alarms since benign clients might occasionally send a few malicious queries.

5.4.2 Impacts of Batch Size

Relying on a single query for identifying adversaries can lead to a significant false alarms due to the limited entropy

TABLE 6
The DAcc., FPR of FDINET to defend against *FeatC*.

Dataset	\hat{F}	JBA		T-RND		Knockoff		ActiveThief		DFME		DaST	
		DAcc.	FPR	DAcc.	FPR	DAcc.	FPR	DAcc.	FPR	DAcc.	FPR	DAcc.	FPR
CIFAR10	VGG11	90.30	6.10	93.10	5.70	51.30	4.70	64.00	6.10	100.0	5.70	98.90	4.70
	ResNet50	91.60	4.00	93.30	3.40	32.10	2.80	43.30	4.00	100.0	3.40	98.70	2.80
GTSRB	VGG11	86.60	0.0	84.50	0.0	99.60	0.0	99.90	0.0	99.90	0.0	100.0	0.0
	ResNet50	86.60	0.0	84.50	0.0	99.80	0.0	100.0	0.0	100.0	0.0	100.0	0.0
CelebA	VGG11	90.40	0.0	91.10	0.0	86.80	0.0	96.30	0.0	100.0	0.0	100.0	0.0
	ResNet50	91.60	0.0	92.30	0.0	87.00	0.0	82.00	0.0	100.0	0.0	100.0	0.0
Skin Cancer	VGG11	90.30	0.0	93.00	0.0	56.40	0.0	76.10	0.0	99.70	0.0	99.30	0.0
	ResNet50	91.20	0.0	92.20	0.0	64.00	0.0	80.30	0.0	100.0	0.0	99.60	0.0

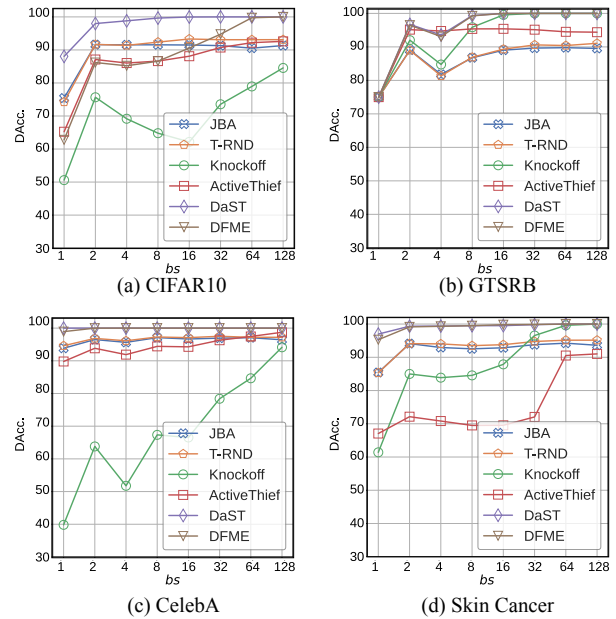
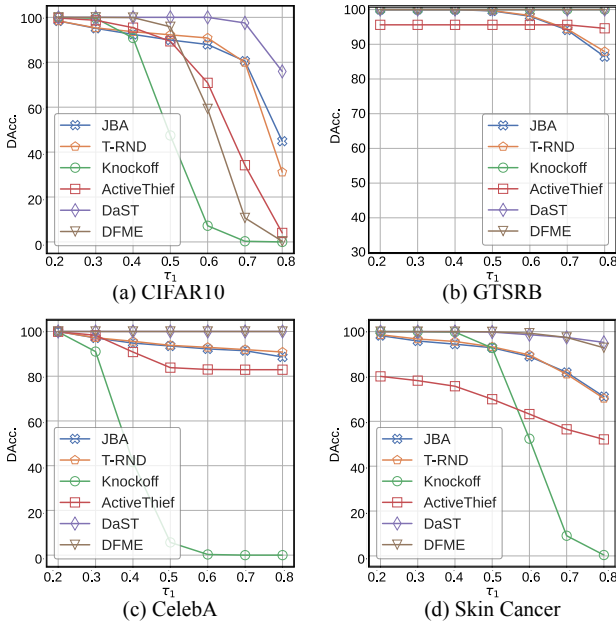


Fig. 6. The performance of FDINET with various thresholds τ_1 .

Fig. 7. The performance of FDINET with various batch size bs .

within the query’s features. To mitigate this, we adopt a majority voting strategy, as explained in Section 4.3. The choice of batch size (bs) plays a crucial role in determining the overall detection accuracy of our approach. In order to assess the performance of our defense, we conduct an empirical evaluation where we examine the effectiveness of our method across a range of batch sizes, specifically from 2 to 128.

Figure 7 illustrates the impact of batch size (bs) on the DAcc. of FDINET. It is evident from the figure that as the batch size increases, the DAcc. also improves. Furthermore, Figure 7 highlights that our defense attains high DAcc. for JBA, T-RND, DFME, and DaST using just 64 queries.

6 DISCUSSION

6.1 Adaptive Attacks

In this section, we explore two specific adaptive attacks: *Feature Correction* and *Dummy Query*. In those attacks, the adversaries know FDINET and potentially modify their attack strategies in order to evade our detection mechanisms.

6.1.1 Feature Correction (*FeatC*)

The adaptive adversary knows our method utilizes the FDI phenomenon to detect malicious queries. Consequently, the adversary can strategically modify the feature maps before submitting them to the MLaaS platform, as discussed in Section 4.4. In this experiment, we make two assumptions about the adversary: (1) the adaptive adversary possesses a pre-trained encoder drawn from the model zoo (VGG11 and ResNet50), and (2) the adversary has access to a mini-batch of training data \mathcal{D}_{train} , which serves as the anchor samples. The adaptive adversary initiates the process by generating 50,000 queries using existing model extraction attacks (such as JBA and T-RND). Subsequently, the adversary applies the L-BFGS optimizer within *FeatC* to re-correct the feature maps associated with these queries.

Table 6 illustrates the performance of FDINET in defending against *FeatC*, where the auxiliary encoders of *FeatC* are VGG11 and ResNet50. However, there is a slight decrease in DAcc. for Knockoff and ActiveThief, as these model extraction techniques employ natural images that may overlap with the training set. Nonetheless, FDINET continues to be effective in defending against the majority of attacks.

TABLE 7
Increased overhead to circumvent FDINET's detection.

Dataset ↓	Attacks →	JBA	T-RND	Knockoff	ActiveThief	DFME	DaST
CIFAR10	Original queries	50,000	50,000	50,000	50,000	50,000	50,000
	Additional queries	128,924	116,910	77,732	96,319	163,709	89,221
	Overhead	+357.85%	+333.82%	+255.46%	+292.64%	+427.42%	+278.44%
GTSRB	Original queries	50,000	50,000	50,000	50,000	50,000	50,000
	Additional queries	120,309	123,705	120,224	129,314	129,720	127,116
	Overhead	+340.62%	+347.41%	+340.45%	+358.63%	+359.44%	+354.23%
CelebA	Original queries	50,000	50,000	50,000	50,000	50,000	50,000
	Additional queries	200,809	199,703	76,032	190,312	219,002	240,634
	Overhead	+501.62%	+499.41%	+252.06%	+480.62%	+538.00%	+581.27%
Skin Cancer	Original queries	50,000	50,000	50,000	50,000	50,000	50,000
	Additional queries	90,621	89,133	75,025	88,424	99,620	96,019
	Overhead	+281.24%	+278.27%	+250.05%	+276.85%	+299.24%	+292.04%

6.1.2 Dummy Query

PRADA introduced the *Dummy Query* attack, an adaptive strategy where the adversary maintains a normal distribution of distances between queries. Although these queries do not contribute to the surrogate model's construction, they serve the purpose of evading detection. It is assumed that the adaptive adversary possesses complete knowledge of the detection algorithm, including the secret detection threshold value τ_1 . With the objective of creating a query set comprising 50,000 samples, the adversary injects benign samples into the submitted queries. In our evaluation, we inject a percentage $p\%$ of benign samples in the submitted queries, with a batch size (bs) set to 50. We incrementally increase p from 0 to 100 in intervals of 10 until the batch queries are predicted as benign by FDINET. Our evaluation provides an estimated lower bound on the number of queries required to evade FDINET detection.

Table 7 shows the increased overhead to circumvent FDINET's detection. The results indicate that our method increases the query overhead ranging from +252.06% to +581.27%. This experiment serves as evidence that, despite the adaptive adversary's ability to distribute queries among multiple clients to evade detection, our method can still enhance its query budget at least $\times 2.5$ times.

6.2 Limitations and Future Work

Language model. This paper primarily focuses on empirical studies conducted in the field of computer vision. However, it is crucial to recognize the significant advancements achieved in language model development. Prominent pre-trained language transformers, including BERT and GPT-3, have been extensively employed in various downstream applications. Nonetheless, these models are still under the threat of model extraction attacks [7], [63]. We believe that our proposed method is able to transfer to language models. In the future, we plan to extend this research to encompass language models and devise a novel model extraction detector approach specifically designed for the NLP domain.

7 CONCLUSION

This paper introduces FDI, a metric that quantitatively measures the deviation in the feature distribution of incoming

queries. Through FDI, we develop both an extraction attacks detector and a colluding adversaries detector. Extensive experiments demonstrate the effectiveness and efficiency of FDINET in detecting extraction attacks. Furthermore, FDINET exhibits robustness in identifying stealthiness attacks, including distributed attacks, *Dummy Query*, and *Feature Correction*. We hope this research can contribute to building a more secure MLaaS platform and promoting the scientific community's awareness of defending against model extraction attacks.

REFERENCES

- [1] H. Zhang, Y. Li, Y. Huang, Y. Wen, J. Yin, and K. Guan, "Mlmod-elastic: An automatic cloud platform for efficient mlaas," in *Proceedings of the 28th ACM International Conference on Multimedia*, 2020, pp. 4453–4456.
- [2] "Machine learning as a service market size," <https://www.mordorintelligence.com/industry-reports/global-machine-learning-as-a-service-mlaas-market>, accessed: 2023-05-30.
- [3] F. Tramèr, F. Zhang, A. Juels, M. K. Reiter, and T. Ristenpart, "Stealing machine learning models via prediction apis," in *25th {USENIX} Security Symposium ({USENIX} Security 16)*, 2016, pp. 601–618.
- [4] M. Jagielski, N. Carlini, D. Berthelot, A. Kurakin, and N. Papernot, "High accuracy and high fidelity extraction of neural networks," in *29th USENIX Security Symposium (USENIX Security 20)*, 2020, pp. 1345–1362.
- [5] Y. Shen, X. He, Y. Han, and Y. Zhang, "Model Stealing Attacks Against Inductive Graph Neural Networks," in *SP 2022 - 43rd IEEE Symposium on Security and Privacy*. San Francisco, United States: IEEE, May 2022, pp. 1–22.
- [6] Z. Sha, X. He, N. Yu, M. Backes, and Y. Zhang, "Can't steal? contrastive stealing attacks against image encoders," *arXiv preprint arXiv:2201.07513*, 2022.
- [7] K. Krishna, G. S. Tomar, A. P. Parikh, N. Papernot, and M. Iyyer, "Thieves on sesame street! model extraction of bert-based apis," in *8th International Conference on Learning Representations, ICLR 2020, Addis Ababa, Ethiopia, April 26-30, 2020*.
- [8] X. Gong, Q. Wang, Y. Chen, W. Yang, and X. Jiang, "Model extraction attacks and defenses on cloud-based machine learning models," *IEEE Communications Magazine*, vol. 58, no. 12, pp. 83–89, 2020.
- [9] R. Shokri, M. Stronati, C. Song, and V. Shmatikov, "Membership inference attacks against machine learning models," in *2017 IEEE Symposium on Security and Privacy (SP)*. IEEE, 2017, pp. 3–18.
- [10] N. Papernot, P. McDaniel, I. Goodfellow, S. Jha, Z. B. Celik, and A. Swami, "Practical black-box attacks against machine learning," in *Proceedings of the 2017 ACM on Asia conference on computer and communications security*, 2017, pp. 506–519.

- [11] M. Zhou, J. Wu, Y. Liu, S. Liu, and C. Zhu, "Dast: Data-free substitute training for adversarial attacks," in *Proceedings of the IEEE/CVF Conference on Computer Vision and Pattern Recognition*, 2020, pp. 234–243.
- [12] W. Wang, B. Yin, T. Yao, L. Zhang, Y. Fu, S. Ding, J. Li, F. Huang, and X. Xue, "Delving into data: Effectively substitute training for black-box attack," in *Proceedings of the IEEE/CVF Conference on Computer Vision and Pattern Recognition*, 2021, pp. 4761–4770.
- [13] C. Ma, L. Chen, and J.-H. Yong, "Simulating unknown target models for query-efficient black-box attacks," in *Proceedings of the IEEE/CVF Conference on Computer Vision and Pattern Recognition*, 2021, pp. 11 835–11 844.
- [14] O. Bastani, C. Kim, and H. Bastani, "Interpreting blackbox models via model extraction," *arXiv preprint arXiv:1705.08504*, 2017.
- [15] D. Kazhdan, B. Dimanov, M. Jamnik, and P. Liò, "Meme: generating rnn model explanations via model extraction," *arXiv preprint arXiv:2012.06954*, 2020.
- [16] M. Kesarwani, B. Mukhoty, V. Arya, and S. Mehta, "Model extraction warning in mlaas paradigm," in *Proceedings of the 34th Annual Computer Security Applications Conference*, 2018, pp. 371–380.
- [17] M. Juuti, S. Szyller, S. Marchal, and N. Asokan, "Prada: protecting against dnn model stealing attacks," in *2019 IEEE European Symposium on Security and Privacy (EuroS&P)*. IEEE, 2019, pp. 512–527.
- [18] A. M. Sadeghzadeh, F. Dehghan, A. M. Sobhanian, and R. Jalili, "Hardness of samples is all you need: Protecting deep learning models using hardness of samples," *arXiv preprint arXiv:2106.11424*, 2021.
- [19] Z. Zhang, Y. Chen, and D. Wagner, "Seat: Similarity encoder by adversarial training for detecting model extraction attack queries," in *Proceedings of the 14th ACM Workshop on Artificial Intelligence and Security*, 2021, pp. 37–48.
- [20] J. Lee, S. Han, and S. Lee, "Model stealing defense against exploiting information leak through the interpretation of deep neural nets," in *Proceedings of the Thirty-First International Joint Conference on Artificial Intelligence (IJCAI)*, 2022.
- [21] S. Kariyappa, A. Prakash, and M. K. Qureshi, "Protecting dnns from theft using an ensemble of diverse models," in *International Conference on Learning Representations*, 2020.
- [22] H. Zheng, Q. Ye, H. Hu, C. Fang, and J. Shi, "Bdpl: A boundary differentially private layer against machine learning model extraction attacks," in *European Symposium on Research in Computer Security*. Springer, 2019, pp. 66–83.
- [23] —, "Protecting decision boundary of machine learning model with differentially private perturbation," *IEEE Transactions on Dependable and Secure Computing*, vol. 19, no. 3, pp. 2007–2022, 2020.
- [24] T. Orekondy, B. Schiele, and M. Fritz, "Prediction poisoning: Towards defenses against DNN model stealing attacks," in *8th International Conference on Learning Representations, ICLR 2020, Addis Ababa, Ethiopia, April 26–30, 2020*, 2020.
- [25] A. Dziedzic, M. A. Kaleem, Y. S. Lu, and N. Papernot, "Increasing the cost of model extraction with calibrated proof of work," in *The Tenth International Conference on Learning Representations, ICLR 2022, Virtual Event, April 25–29, 2022*. OpenReview.net, 2022.
- [26] S. Kariyappa and M. K. Qureshi, "Defending against model stealing attacks with adaptive misinformation," in *Proceedings of the IEEE/CVF Conference on Computer Vision and Pattern Recognition*, 2020, pp. 770–778.
- [27] S. Pal, Y. Gupta, A. Kanade, and S. Shevade, "Stateful detection of model extraction attacks," *arXiv preprint arXiv:2107.05166*, 2021.
- [28] T. Orekondy, B. Schiele, and M. Fritz, "Knockoff nets: Stealing functionality of black-box models," in *Proceedings of the IEEE/CVF Conference on Computer Vision and Pattern Recognition*, 2019, pp. 4954–4963.
- [29] S. Pal, Y. Gupta, A. Shukla, A. Kanade, S. Shevade, and V. Ganapathy, "Activethief: Model extraction using active learning and unannotated public data," in *Proceedings of the AAAI Conference on Artificial Intelligence*, vol. 34, no. 01, 2020, pp. 865–872.
- [30] V. Chandrasekaran, K. Chaudhuri, I. Giacomelli, S. Jha, and S. Yan, "Exploring connections between active learning and model extraction," in *29th {USENIX} Security Symposium ({USENIX} Security 20)*, 2020, pp. 1309–1326.
- [31] J. R. Correia-Silva, R. F. Berriel, C. Badue, A. F. de Souza, and T. Oliveira-Santos, "Copycat cnn: Stealing knowledge by persuading confession with random non-labeled data," in *2018 International Joint Conference on Neural Networks (IJCNN)*. IEEE, 2018, pp. 1–8.
- [32] X. He, J. Jia, M. Backes, N. Z. Gong, and Y. Zhang, "Stealing links from graph neural networks," in *USENIX Security Symposium*, 2021, pp. 2669–2686.
- [33] Y. Wang, H. Qian, and C. Miao, "Dualcf: Efficient model extraction attack from counterfactual explanations," in *2022 ACM Conference on Fairness, Accountability, and Transparency*, 2022, pp. 1318–1329.
- [34] H. Yu, K. Yang, T. Zhang, Y.-Y. Tsai, T.-Y. Ho, and Y. Jin, "Cloudleak: Large-scale deep learning models stealing through adversarial examples," in *Proceedings of Network and Distributed Systems Security Symposium (NDSS)*, 2020.
- [35] A. Barbalau, A. Cosma, R. T. Ionescu, and M. Popescu, "Black-box ripper: Copying black-box models using generative evolutionary algorithms," 2020.
- [36] J.-B. Truong, P. Maini, R. J. Walls, and N. Papernot, "Data-free model extraction," in *Proceedings of the IEEE/CVF Conference on Computer Vision and Pattern Recognition (CVPR)*, June 2021.
- [37] S. Sanyal, S. Addepalli, and R. V. Babu, "Towards data-free model stealing in a hard label setting," in *Proceedings of the IEEE/CVF Conference on Computer Vision and Pattern Recognition*, 2022, pp. 15 284–15 293.
- [38] T. Miura, S. Hasegawa, and T. Shibahara, "Megex: Data-free model extraction attack against gradient-based explainable ai," *arXiv preprint arXiv:2107.08909*, 2021.
- [39] S. Kariyappa, A. Prakash, and M. K. Qureshi, "Maze: Data-free model stealing attack using zeroth-order gradient estimation," in *Proceedings of the IEEE/CVF Conference on Computer Vision and Pattern Recognition*, 2021, pp. 13 814–13 823.
- [40] X. Gong, Y. Chen, W. Yang, G. Mei, and Q. Wang, "Inversenet: Augmenting model extraction attacks with training data inversion," in *Proceedings of the Thirtieth International Joint Conference on Artificial Intelligence, IJCAI 2021, Virtual Event / Montreal, Canada, 19–27 August 2021*, Z. Zhou, Ed. ijcai.org, 2021, pp. 2439–2447.
- [41] Z. Ma, X. Liu, Y. Liu, X. Liu, Z. Qin, and K. Ren, "Divtheft: An ensemble model stealing attack by divide-and-conquer," *IEEE Transactions on Dependable and Secure Computing*, 2023.
- [42] S. Szyller, B. G. Atli, S. Marchal, and N. Asokan, "Dawn: Dynamic adversarial watermarking of neural networks," in *Proceedings of the 29th ACM International Conference on Multimedia*, 2021, pp. 4417–4425.
- [43] H. Jia, C. A. Choquette-Choo, V. Chandrasekaran, and N. Papernot, "Entangled watermarks as a defense against model extraction," in *USENIX Security Symposium*, 2021, pp. 1937–1954.
- [44] N. Lukas, Y. Zhang, and F. Kerschbaum, "Deep neural network fingerprinting by conferrable adversarial examples," 2021.
- [45] Y. Chen, C. Shen, C. Wang, and Y. Zhang, "Teacher model fingerprinting attacks against transfer learning," in *31st USENIX Security Symposium (USENIX Security 22)*, 2022, pp. 3593–3610.
- [46] X. Pan, Y. Yan, M. Zhang, and M. Yang, "Metav: A meta-verifier approach to task-agnostic model fingerprinting," in *Proceedings of the 28th ACM SIGKDD Conference on Knowledge Discovery and Data Mining*, 2022, pp. 1327–1336.
- [47] P. Maini, M. Yaghini, and N. Papernot, "Dataset inference: Ownership resolution in machine learning," in *9th International Conference on Learning Representations, ICLR 2021, Virtual Event, Austria, May 3–7, 2021*. OpenReview.net, 2021.
- [48] A. Dziedzic, H. Duan, M. A. Kaleem, N. Dhawan, J. Guan, Y. Cattan, F. Boenisch, and N. Papernot, "Dataset inference for self-supervised models," *arXiv preprint arXiv:2209.09024*, 2022.
- [49] L. Zhu, Y. Li, X. Jia, Y. Jiang, S.-T. Xia, and X. Cao, "Defending against model stealing via verifying embedded external features," in *ICML 2021 Workshop on Adversarial Machine Learning*, 2021.
- [50] Y. Li, L. Zhu, X. Jia, Y. Jiang, S.-T. Xia, and X. Cao, "Defending against model stealing via verifying embedded external features," in *Proceedings of the AAAI Conference on Artificial Intelligence*, vol. 36, no. 2, 2022, pp. 1464–1472.
- [51] E. Quiring, D. Arp, and K. Rieck, "Forgotten siblings: Unifying attacks on machine learning and digital watermarking," in *2018 IEEE European Symposium on Security and Privacy (EuroS&P)*. IEEE, 2018, pp. 488–502.
- [52] T. Lee, B. Edwards, I. Molloy, and D. Su, "Defending against neural network model stealing attacks using deceptive perturbations," in *2019 IEEE Security and Privacy Workshops (SPW)*. IEEE, 2019, pp. 43–49.
- [53] J. Chen, C. Wu, S. Shen, X. Zhang, and J. Chen, "Das-ast: Defending against model stealing attacks based on adaptive softmax transformation," in *International Conference on Information Security and Cryptology*. Springer, 2020, pp. 21–36.

- [54] A. Dziedzic, M. A. Kaleem, Y. S. Lu, and N. Papernot, "Increasing the cost of model extraction with calibrated proof of work," in *10th International Conference on Learning Representations, ICLR, 2022*.
- [55] M. Mazeika, B. Li, and D. Forsyth, "How to steer your adversary: Targeted and efficient model stealing defenses with gradient redirection," in *International Conference on Machine Learning*. PMLR, 2022, pp. 15 241–15 254.
- [56] A. Krizhevsky, G. Hinton *et al.*, "Learning multiple layers of features from tiny images," 2009.
- [57] J. Stallkamp, M. Schlipsing, J. Salmen, and C. Igel, "Man vs. computer: Benchmarking machine learning algorithms for traffic sign recognition," *Neural networks*, vol. 32, pp. 323–332, 2012.
- [58] Z. Liu, P. Luo, X. Wang, and X. Tang, "Large-scale celebfaces attributes (celeba) dataset," *Retrieved August*, vol. 15, no. 2018, p. 11, 2018.
- [59] N. Codella, V. Rotemberg, P. Tschandl, M. E. Celebi, S. Dusza, D. Gutman, B. Helba, A. Kalloo, K. Liopyris, M. Marchetti *et al.*, "Skin lesion analysis toward melanoma detection 2018: A challenge hosted by the international skin imaging collaboration (isic)," *arXiv preprint arXiv:1902.03368*, 2019.
- [60] L. N. Darlow, E. J. Crowley, A. Antoniou, and A. J. Storkey, "Cinic-10 is not imagenet or cifar-10," *arXiv preprint arXiv:1810.03505*, 2018.
- [61] G. B. Huang, M. Mattar, T. Berg, and E. Learned-Miller, "Labeled faces in the wild: A database for studying face recognition in unconstrained environments," in *Workshop on faces in 'Real-Life' Images: detection, alignment, and recognition*, 2008.
- [62] M. Combalia, N. C. Codella, V. Rotemberg, B. Helba, V. Vilaplana, O. Reiter, C. Carrera, A. Barreiro, A. C. Halpern, S. Puig *et al.*, "Bcn20000: Dermoscopic lesions in the wild," *arXiv preprint arXiv:1908.02288*, 2019.
- [63] S. Zanella-Beguelin, S. Tople, A. Paverd, and B. Köpf, "Grey-box extraction of natural language models," in *International Conference on Machine Learning*. PMLR, 2021, pp. 12 278–12 286.